A Fundamental Comparison of Canard and Conventional Configurations

Tad McGeer* and Ilan Kroo†
Stanford University, Stanford, California

This paper examines the relative efficiency of canard, tandem, and aft-tailed aircraft configurations through analysis of an elementary lifting system. Stability and trim requirements are imposed upon the system and its $C_{L_{max}}$, drag, and structural weight are studied as its geometry varies over a wide range of possible configurations. During the course of the analysis, two general solutions emerge for minimum induced drag as a function of the geometry and the division of lift between the surfaces of such a system—one for fixed span and the other for fixed weight. The conclusion is that the pre-eminence of the conventional aft-tailed configuration has a sound fundamental basis, but that there may be some room for improvement.

Introduction

OVER the eighty years since the Wrights first demonstrated a canard design, one might have expected some consensus to emerge on the utility of such unconventional configurations. But debate continues, particularly in general aviation circles, between those who accept the conventional aft-tailed arrangement of lifting surfaces and those who feel that canards, or even tandems, should have wider application. Ultimate resolution of this issue remains elusive, since the number of potential applications is large and the factors common to all tend to be obscured by concentration upon specific cases. This paper addresses the debate in a more general way. Our strategy is to strip the competing configurations down to their simplest form—an elementary system of two lifting surfaces. We impose stability and trim requirements upon this system, and then study its performance while varying its geometry over the entire spectrum from conventional to tandem and canard arrangements. Considered first are the trimmed $C_{L_{max}}$ and induced drag, first with fixed span and then with fixed area and structural weight. Then the geometries are compared on the basis of total drag for a given weight and stall speed. In taking this approach, many details of particular applications are excluded, but the trends that emerge are always present and are always powerful—except, perhaps in low-aspect-ratio or supersonic configurations, which presumably are not designed with efficiency as the uppermost objective.

Stability and Balance

The performance of any lifting system depends critically upon the sharing of lift between the surfaces. In practice, stability and balance constraints determine this sharing. These therefore dictate a three-step approach to the analysis of any system: 1) location of the center of gravity (c.g.) to give the desired stability level; 2) distribution of the lift between the two surfaces to balance the system; and 3) determination of the consequences of that lift distribution. To formulate this approach quantitatively, some terms need to be defined. We refer to the tail as the surface of smaller span, regardless of whether or not it is behind the wing. If l is the distance between the aerodynamic centers (a.c.) of the two surfaces, then $\bar{l}_T$ is the distance from c.g. to tail a.c./l, $\bar{S}_T$ the tail area/total area, $\bar{L}_T$ the tail lift/total lift, and $C_{L\alpha_T}$ the tail lift curve slope, with C_{L_T} based upon the tail area. A similar set with subscript W applies to the wing. $\bar{l}_W$ and $\bar{l}_T$ are positive when the corresponding surface a.c.'s are aft of the c.g. We also need a system C_L based upon total area and C_M based upon some mean chord $\bar{c}$. The stability and balance relations are then

$$\text{Stability:}\quad C_{M\alpha} \sim -(C_{L\alpha_W}\bar{S}_W\bar{l}_W + C_{L\alpha_T}\bar{S}_T\bar{l}_T)$$

$$\text{Balance:}\quad C_M \sim -(\bar{L}_W\bar{l}_W + \bar{L}_T\bar{l}_T) + \frac{C_{M_O}\bar{c}}{C_L l}$$

(C_{M_O} as used here has an unconventional definition—normally it would include both the intrinsic pitching moment of each surface *about* its a.c. and the couple due to lift acting *through* the two a.c.'s. We have extracted the latter and written it explicitly.) The neutral point can be located by setting $C_{M\alpha}$ to zero in the stability equation. To provide a stability margin, the c.g. is placed ahead of the neutral point by a distance Δ (normalized by l); this distance is therefore added to the corresponding $\bar{l}_W$ and $\bar{l}_T$. Substituting these into the balance equation gives the tail lift fraction,

$$\bar{L}_T = \frac{\bar{S}_T}{\bar{S}_T + \dfrac{C_{L\alpha_W}}{C_{L\alpha_T}}\bar{S}_W} \mp \Delta \pm \frac{C_{M_O}\bar{c}}{C_L l}$$

The upper set of signs applies for an aft tail and the lower for a canard. Disregarding for the present the effects of C_{M_O} and the interference between the surfaces, observe that the tail lift fraction is the same for aft-tailed and canard systems having the same tail area but *opposite* stability margin. This symmetry can best be understood by considering the effect of reversing the flow over a system. (For simplicity, suppose each surface to be an unswept lifting line.) Neither the c.g. nor the a.c.'s move, so Δ simply changes sign with the flow direction and the lift fractions are unaffected. Now, if these remain fixed, total drag, weight, and $C_{L_{max}}$ are for the most part independent of the streamwise positions of the surfaces; hence, a canard system will have nearly the same performance as an aft-tailed system with opposite stability.

But what about C_{M_O} and interference between the surfaces? Since system performance is sensitive to tail load only at rather high C_L and since the effect of C_{M_O} upon tail load diminishes with increasing C_L, C_{M_O} is normally a minor factor—at least with flaps up. Hence, C_{M_O} is neglected in our calculations. (However, the potential effects of nonzero C_{M_O}—which are not always small, particularly with flaps down—will become apparent as we proceed.) On the other hand, interference has a significant effect. The velocities induced in a canard system make the wing's lift curve slope lower, and the tail's higher, than in a system having an aft tail of the same size. A lower ($C_{L\alpha_W}/C_{L\alpha_T}$) implies a higher $\bar{L}_T$; a compensating reduction in Δ is required to get the *same* tail load in the canard system. Effectively, this is just a shift (typically about -0.05 in Δ) in our basic symmetrical picture.

Submitted Sept. 10, 1982; revision received Feb. 18, 1983.

*Research Assistant, Department of Aeronautics and Astronautics. Student Member AIAA.
†Research Assistant, Department of Aeronautics and Astronautics. Presently at NASA Ames Research Center.

Consequently, we can concentrate upon stable systems. Then, just by transposing the results for canards and aft tails—and making some allowance for downwash—we can obtain those for unstable systems as well.

To proceed, a method for calculating $(C_{L\alpha_W}/C_{L\alpha_T})$ is needed. We have applied a lifting line method in which each surface is represented by a single bound vortex trailing a flat vortex sheet parallel to the freestream. This calculation is affected most strongly by the tail area fraction $\bar{S}_T$ and tail-to-wing span ratio $\bar{b}_T$. Other parameters—for example, the aspect ratio of the system (b_W^2/S_{total}) and the vertical and streamwise gaps between the surfaces—have such a weak effect that variations ove the range of reasonable values change $\bar{L}_T$ only slightly. Consequently, a typical set gives values of $(C_{L\alpha_W}/C_{L\alpha_T})$ that are applicable over broad range: used here are a system aspect ratio of 8, a vertical gap of $0.1b_W$, and a streamwise gap of $4\bar{c}$. Sweep also affects loadings, not only by changing $(C_{L\alpha_W}/C_{L\alpha_T})$ but also by introducing, in combination with surface twist, an additional source of pitching moment. For aft-tailed systems the change in $(C_{L\alpha_W}/C_{L\alpha_T})$ is generally slightly beneficial, while for canards it is insignificant; in any case, the tail loads change little with sweep. Similarly, the moment due to sweep is normally too small to have a significant influence on trim. Therefore, only unswept surfaces are considered here.

Δ must also be specified. A representative value is 0.1. This would correspond to a fairly large static margin (40%, with $l=4\bar{c}$) if no other effects were present, but in actuality destabilizing contributions from other parts of the airframe reduce the margin somewhat. Furthermore, since the calculated tail loads exclude the contribution of $C_{M_{\sim}}$, they are

Maximum Lift in Trim

This outline completes discussion of the first two steps of our analytical procedure: locating the c.g. and balancing the system. The rest of the paper is devoted to the third step: determining the consequences. Consider first the consequences for $C_{L_{\max}}$. Suppose the two surfaces of the system have the same *potential* maximum C_L, denoted by $C_{l_{\max}}$. Then what maximum overall C_L can be reached, in trim, before one of the surfaces stalls? Moreover, how does the trimmed $C_{L_{\max}}$ vary with the system geometry? Figure 1 illustrates the variation in trimmed $C_{L_{\max}}$ over the whole continuum of lifting systems. Canard systems, which we define as having the shorter span in front regradless of its area, are on the left. Aft-tailed systems (also broadly defined) are on the right. The ordinate is the fraction of $C_{l_{\max}}$ that the system can achieve in trim. Its calculation is straightforward: evaluate (C_L/C_{L_T}) using the tail lift equation and (C_L/C_{L_W}) with the corresponding formula for the wing; $(C_{L_{\max}}/C_{l_{\max}})$ is the lower of the two.

Observe that, for any division of area between the front and rear surfaces, there is some span ratio that makes their C_L's equal, and the full potential $C_{L_{\max}}$ is realized. In a stable system this happens when the forward surface has a lower lift curve slope than the rear—that is, when it has a lower aspect ratio and, hence, a smaller span (particularly since the interaction between the surfaces drives the lift curve slopes in the opposite direction). In fact, the systems with the highest $C_{L_{\max}}$ all have roughly the same "aspect ratio ratio," i.e., the optimum $\bar{b}_T$ varies roughly with $\sqrt{\bar{S}_T}$. Now, if the forward surface's span is reduced from the optimum, then the ratio of rear-to-forward lift curve slopes increases, the neutral point moves aft, the c.g. follows it to maintain the stability level, the rear surface's C_L increases to maintain balance—and it stalls first. Fortunately, systems having this very dangerous characteristic occupy only the small fraction of design space to the left of the $C_{L_{\max}}$ peaks in Fig. 1. On the other hand, if the span ratio increases, the process reverses. Ultimately, as the forward surface grows into a wing and the rear surface becomes a small tail, the c.g. moves ahead of the wing. The

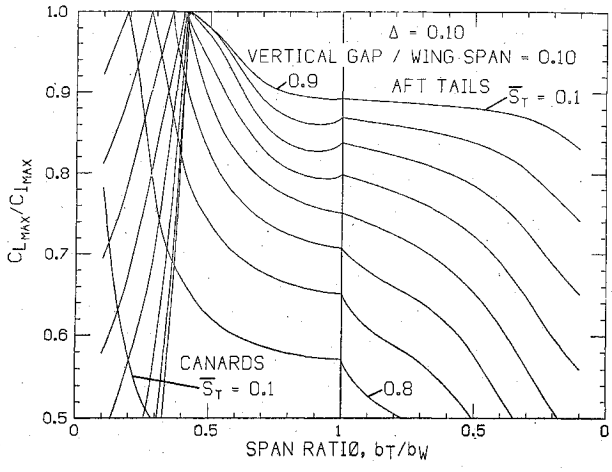

Fig. 1 Relative maximum lift of trimmed systems.

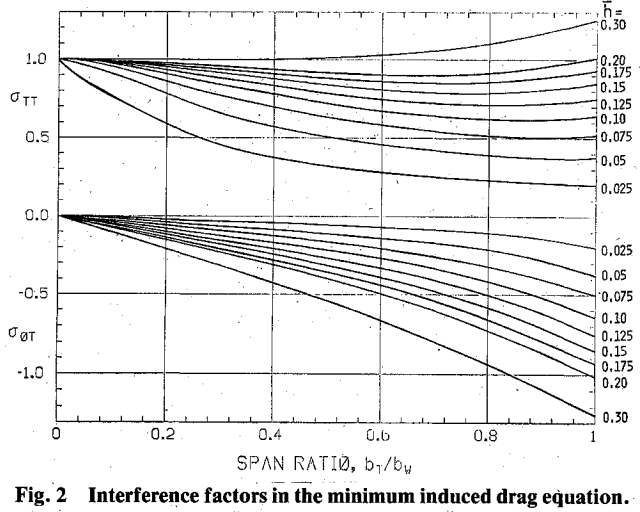

Fig. 2 Interference factors in the minimum induced drag equation.

tail must then be downloaded for balance. With further reduction in tail size, the download becomes the limiting factor—the rear surface stalls first in the negative sense. Systems with this problem also occupy a small region in the design space: all have tail span ratios less than 0.1 when $\Delta=0.1$.

The $C_{L_{\max}}$ available at the optimum points is certainly attractive, but the accompanying sensitivity to Δ, C_{M_O}, and changes in geometry is intimidating. Unfortunately, (unless the stability is almost neutral) the two characteristics go together. For high $C_{L_{\max}}$, a system must have a forward surface of relatively low aspect ratio, yet fundamental aerodynamics dictate that the ratio of lift curve slopes, and therefore, the neutral point in such a system is quite sensitive to changing surface dimensions. ($C_{L_{\max}}$ varies considerably among systems with very small aft tails for the same reason.) Moreover, the small forward surface area compounds the problem, since a shift in the neutral point requires changes in surface lift fractions that are independent of area; hence, the smaller the area, the larger the corresponding changes in surface C_L. Of course, a change in Δ has the same effect as a shift in the neutral point. Thus, for example, if Δ increases to 0.15, then the $C_{L_{\max}}$ of a canard system with $\bar{S}_T=0.2$ decreases by about 15% over the range of span ratios; with an aft tail of the same size, the drop is only about 5%.

Before drawing conclusions from the results of Fig. 1, we should ask a further question. Often both surfaces do not have the same potential $C_{L_{\max}}$—most notably because about one-quarter of the larger span is normally reserved for ailerons, while the smaller surface can have full span flaps. The *potential* $C_{L_{\max}}$ of a wing is therefore somewhat lower

than that of a tail. How would that change Fig. 1? Again the calculation is straightforward. If the system's $C_{L_{max}}$ is referenced to that of a *fully flapped* surface, then we need only multiply (C_L/C_{L_W}) and (C_L/C_{L_T}) from the previous analysis by the fraction of fully flapped $C_{l_{max}}$ that each surface can achieve, and again take the lower of the two. Then on the right side of the figure, where the wing stalls first, everything will simply be reduced by $(C_{L_{W_{max}}}/C_{l_{max}})$. On most of the left side there will be no change, except that the curves on which the canard is critical will be cut off by wing stall at a lower $(C_{L_{max}}/C_{l_{max}})$. The cutoff still occurs when both surfaces reach their respective $C_{L_{max}}$ simultaneously; therefore at

$$\left(\frac{C_{L_{max}}}{C_{l_{max}}}\right)=\bar{S}_T+\frac{C_{L_{W_{max}}}}{C_{l_{max}}}\bar{S}_W$$

For example, the $C_{l_{max}}$ of an unflapped section of the wing is typically 0.6 that of a flapped section; if we take one-quarter of the wing area to be unflapped, then simple weighting by the area fraction gives $(C_{L_{W_{max}}}/C_{l_{max}})=0.9$. The $C_{l_{max}}$ of the aft-tailed systems would therefore be reduced by 10% across the board, while the canard curves would be cut off at $C_{L_{max}}$ ranging from 0.92 with $\bar{S}_T=0.2$ to 0.98 with $\bar{S}_T=0.8$.

Changes of this magnitude leave the basic character of the results unchanged; their message therefore remains clear: if maximum lift were an end in itself, one would like to make the area of the forward surface much larger, and the span somewhat less, than that of the rear. But there are obvious practical objections to such a configuration. Realistically, then, the choice would be between a system having an aft tail of reasonable size or a more modest canard. On the one hand, the aft tailed system offers a reliable but suboptimal $C_{L_{max}}$. On the other hand, a canard arrangement has the potential for higher $C_{L_{max}}$, but if other factors (principally drag, weight, and the need for a useful c.g. range) dictate changes from the optimum geometry, then the $C_{L_{max}}$ will be unimpresive. Consequently, the question cannot be resolved without bringing these other factors into the analysis.

Minimum Induced Drag with Fixed Span

The first of these factors is trimmed induced drag. While our analysis of $C_{L_{max}}$ was concerned only with the overall lift carried by each surface, in analyzing induced drag the spanwise loading must be considered as well. The immediate goal is to find those spanwise lift distributions that *minimize* induced drag as a function of the tail span ratio, vertical gap between the surfaces, and the sharing of lift between the two surfaces.

A General Solution

This analysis, which is familiar in the case of an isolated wing, becomes more difficult for a lifting system since interference between the surfaces can have a substantial effect—but perhaps not so difficult as one might initially think. Munk's classical stagger theorem[1] affords considerable simplification. The theorem states that the surfaces of a system can be moved relative to each other in the streamwise direction without changing the total drag, provided that their spanwise lift distributions remain fixed. (Of course, one would have to change their geometry while sliding them streamwise to preserve the lift distributions, but that need not concern us now.) A brief physical justification is that the drag depends only upon the amount of energy left in the flow after the transit of the lifting system, and not upon the history of how it is deposited. This theorem eliminates all streamwise parameters from the analysis—not only the gap, but also chord distributions and sweep. The remaining variables are the vertical gap, the surface spans, the lift on the two surfaces, and, of course, their lift distributions.

One approach to the drag calculation involves specifying the lift distributions a priori, and then using a Trefftz plane analysis to find the dependence upon the other parameters. This approach is embodied in Prandtl's classical "biplane equation," which applies when both surfaces are elliptically loaded. But this solution is not quite what we want, since it gives neither the minimum drag that can be achieved nor that is likely to be achieved in practice. One can demonstrate this by considering a system having zero vertical gap and one surface of smaller span than the other. According to the stagger theorem, since there is no gap, this system would have the same drag as a single wing carrying the sum of the lift distributions over the two surfaces. This implies that minimum drag is realized when the sum is elliptic. Hence, if the smaller surface is elliptically loaded, the optimum span loading for the rear surface can be found by subtracting this ellipse from the desired aggregate ellipse—and the result is definitely *not* elliptical. In fact, in canard systems, the downwash directly behind the canard and the upwash outboard tend to perform the subtraction; hence, their induced drag is normally lower in practice than the biplane equation indicates.[2]

Valuable insight can be obtained by considering the physics of this example system. Suppose that the smaller span carried all of the lift. In isolation it would generate a drag larger than that of the system by a factor of $(1/\bar{b}_T^2)$. How, then, can there be no drag penalty when it is part of the lifting system, regardless of the lift it carries? Apparently, no matter how much momentum is imparted to the relatively small mass flow within the smaller span's purview, by appropriately loading the wing (even if it carries no net lift), the momentum can—at least in principle—always be redistributed over a wider field. But this is true only when the vertical gap is zero. What if it is not? Nonzero gap is a doubled-edged sword—it increases the mass flow through the system and thus offers the possibility of reducing the drag. However, it also reduces the wing's ability to compensate for any excessive loading of the smaller surface.

To determine quantitatively the potential gains and losses, the minimum induced drag problem must be solved—which involves finding the optimum span loadings. This approach has been taken in special cases by Blackwell[3] and Lamar.[4] Butler[5] and Kroo[6] have presented equivalent solutions for the optimum lift distribution for the larger span, and the corresponding system drag, with fixed elliptic loading on the smaller span. Their result is in fact quite close to the true optimum solution for two surface systems in subsonic flow, which can be presented in the following form. (See Appendix A for development.) The optimum lift distributions are functions of $\bar{L}_T$, $\bar{b}_T$, and the vertical gap $\bar{h}$ normalized by b_W. The drag obtained with these lift distributions is given by the following quadratic in the tail lift fraction:

$$D_i=\frac{L^2}{\pi q b_W^2}\left(\sigma_0+\frac{\sigma_{0T}}{\bar{b}_T}\bar{L}_T+\frac{\sigma_{TT}}{\bar{b}_T^2}\bar{L}_T^2\right) \tag{1}$$

where L is the total lift and q the dynamic pressure. The σ's are interference factors, which are only functions of $\bar{b}_T$ and $\bar{h}$. σ_{0T} and σ_{TT} are plotted in Fig. 2. We have not plotted σ_0 because it is almost unity except when $\bar{b}_T$ is large and $\bar{h}$ moderate; an extreme case is $\bar{b}_T=1$, $\bar{h}=0.05$, for which σ_0 is 0.98. It should be noted that, while one often distinguishes between self-induction and interference terms in a formula such as this, each term here includes both effects.

The interference factors given in Fig. 2 were calculated using the familiar vortex sheet model, but the calculation can also be made with the forward surface's wake "rolled up" into two discrete vortices. The drag is only weakly dependent upon the assumed spanwise position of the tip vortices, and over the interesting ranges of $\bar{L}_T$, $\bar{b}_T$, and $\bar{h}$ differs by no more than a few percent from that obtained with a flat wake model. Hence, the solution is apparantly insensitive to wake geometry.

The quantity in parentheses in Eq. (1) is commonly denoted by $(1/u)$, u being the so-called span efficiency. $(1/u)$ is the

ratio of the system's drag to that of an elliptically loaded wing having the same span and total lift. If the gap is zero, then according to Munk's stagger theorem it is always unity. But as we argued earlier, the situation is entirely different when the gap is finite. Figure 3 is a plot of $(1/u)$ vs span ratio and lift fraction for two gaps—a quite minimal 0.025 and 0.1 (between those of typical low and T-Tails). It shows that the drag is indeed reduced if the tail carries a near-optimal share of the lift; but unless the span ratio is nearly unity, the optimum tail load and the associated drag reduction are very small. On the other hand, if the tail carries much more than the optimum load, there is a substantial drag penalty. As the gap becomes larger, the stakes increase. Thus, making the gap finite in a system with nonoptimal tail loading can have unpleasant consequences. Unfortunately, there is not much choice in practice—even if zero gap could be maintained despite downwash, roll-up, etc., the effect of reduced dynamic pressure upon the rear surface would overwhelm any hoped-for improvement in efficiency. So, practically speaking, drag penalties are inevitable when large loads are carried on small surfaces. (There appears to be a bright spot in this gloom. Note that, if the tail span ratio is near unity, the drag can be reduced relative to that of the wing acting alone, even if the tail carries no *net* lift! Sadly, this surprising result is of only academic interest—the improvement is tiny and the configuration impractical.)

Figure 4 shows a couple of examples of the lift distributions for minimum induced drag. One is a system in which almost all of the lift is carried by the wing—in an essentially elliptical distribution. In the other, a large fraction of the lift is carried by the tail and the wing's lift is sloshed outboard to compensate. However, since the gap is nonzero in this case , the sum of the lift distributions is not elliptical and the drag is much higher than that of an isolated wing. The observant reader will note the unusual scaling of the spans in this figure. Figure 4 is scaled so that the systems would have the same structural weight, a subject to be considered later.

Induced Drag in Trim

First, the trimmed induced drags of systems are to be compared with equal wing spans. To proceed, the drag formula must be combined with the trimmed tail loads from the $C_{L_{max}}$ analysis. The results are plotted in Fig. 5. It is immediately apparent from this figure that small span canards have a most unhealthy effect upon induced drag. Small aft tails, on the other hand, are sometimes beneficial though their effect upon drag is slight unless the span ratio is very low. Of course, this is simply due to the heavier loading on canards compared to most aft tails. In turn, this difference is due almost entirely to the opposite signs on the Δ term in the tail lift equation, although the effect of induced velocities on lift curve slopes has some role. High tail loads are advantageous only if the span ratio is large; hence, the relative positions of canards and aft tails reverse in the large $\bar{b}_T$ range. It is also apparent that trimmed induced drag varies much more among canard than aft-tailed systems. In part, this is because the neutral point in canard systems is more sensitive to changes in geometry (a difference that is ultimately due to the effect of downwash). But the more important reason is that induced drag varies more rapidly with tail load as the tail load increases; therefore, the effect of shifts in the neutral point is relatively pronounced with a canard arrangement. For the same reason, a canard system is more sensitive to changes in Δ and C_{M_O} than is its aft-tailed counterpart.

Now what emerges when the results in Fig. 5 are considered together with the $C_{L_{max}}$ calculations? Most obviously, that $C_{L_{max}}$ and induced drag have a conflict of interest among canards of modest span. For minimum drag one wants a low tail load and, therefore, since $\bar{L}_T$ decreases with $\bar{S}_T$, a small canard (in fact, too small for control). However, $\bar{L}_T$ does not decrease as *rapidly* as $\bar{S}_T$, so a small canard has a high (C_{L_T}/C_L). That, in turn, limits $C_{L_{max}}$. Taken together, each dictates changes from the geometry that is best for the other, and their high sensitivity to such changes makes the resulting compromise unattractive. With an aft tail, on the other hand, there is little conflict.

Putting all preconceptions aside, we can conclude the following from the analysis to this point: a system with a small canard is certainly no the optimum. *Nor*, indeed, is the leading candidate one with a small aft tail. Rather, the apparent optimum is a tandem! Why, then, in the menagerie of modern aircraft, do such configurations comprise a decidedly small minority? The reason, of course, is that their advantages in $C_{L_{max}}$ and span efficiency are generally offset by another factor: structural weight. The next step, therefore, must bring weight into the analysis.

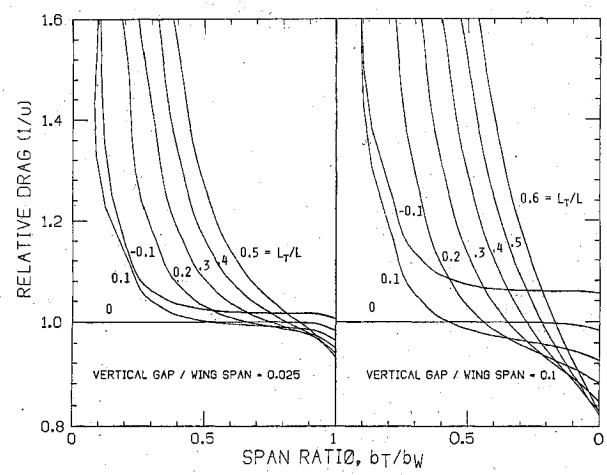

Fig. 3 Minimum induced drag vs tail span ratio and lift fraction.

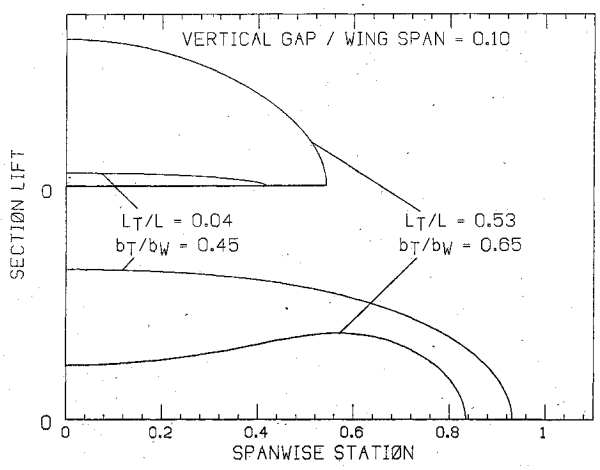

Fig. 4 Lift distributions for maximum span efficiency.

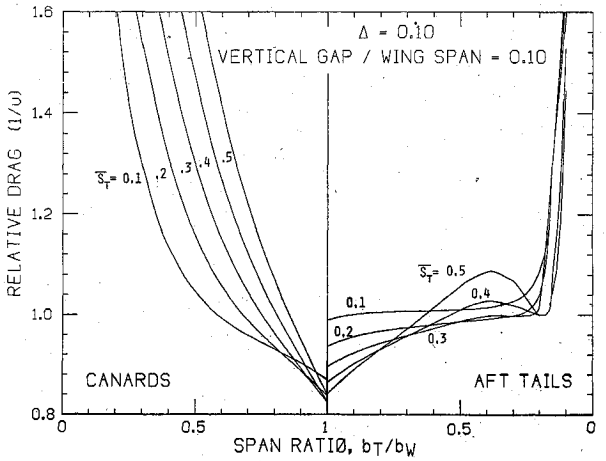

Fig. 5 Relative induced drag of trimmed systems with equal wing spans.

Structural Weight of Lifting Systems

At this point, a method for calculating the relative structural weight of lifting systems is needed. One can easily list a multitude of factors that should have some bearing upon this calculation; however, here as throughout the analysis, we are interested only in those factors having the strongest influence. Consider a cantilever surface of at least moderate aspect ratio—the primary factors affecting its weight are its span, area, and total lift, its thickness, and its lift distribution. We can capture all of these effects by employing the elementary concept of a lifting surface as a Bernoulli-Euler beam. If this concept is applied to a surface having constant thickness ratio and bending stress across the span, the weight per unit span can be written as

$$\frac{dW}{dy} = \frac{w_S S}{b}\chi(y) + \frac{w_b b}{S}\frac{M(y)}{\chi(y)}$$

where $\chi(y)S/b$ is the local chord (for each surface in the lifting sytem, chord is normalized by the surface span and the *total* area) and $M(y)$ the local bending moment. The terms account roughly for the weight of the skin and spar, respectively. Stress levels, thickness, etc., are absorbed by the constants w_S and w_b. To find the total weight of the system, this formula must be integrated across the two spans. The "skin" term simply integrates to $(w_S S)$. The "spar" term is most easily treated by decomposing the local moment into a sum of harmonics, as follows. First, the lift distribution over each surface is expressed as a Fourier series of the form

$$l_W(\theta_W) = \frac{2L}{b_W}\sum_{\text{odd}}^{M} A_{W_m}\sin(m\theta_W)$$

$$l_T(\theta_T) = \frac{2L}{b_T}\sum_{\text{odd}}^{N} A_{T_n}\sin(n\theta_T)$$

where θ_W and θ_T are related to y by

$$y = \frac{b_W}{2}\cos(\theta_W) = \frac{b_T}{2}\cos(\theta_T)$$

Integrating each harmonic of the lift distribution gives a distinct contribution to the bending moment at θ. Define the integral as

$$\mathfrak{M}_m(\theta) \equiv \int_0^{\theta} \sin(m\theta')\sin(\theta')\,[\cos(\theta') - \cos(\theta)]\,d\theta'$$

Then the sum of the harmonic contributions may be written as

$$M_W(\theta_W) = \frac{b_W L}{2}\sum_{\text{odd}}^{M} A_{W_m}\mathfrak{M}_m(\theta_W)$$

$$M_T(\theta_T) = \frac{b_T L}{2}\sum_{\text{odd}}^{N} A_{T_n}\mathfrak{M}_n(\theta_T)$$

and the integral for the "spar" weight becomes

$$W_b = \frac{w_b L}{2}\frac{b_W^3}{S}\left[\sum_{\text{odd}}^{M} A_{W_m}\int_0^{\pi/2}\frac{\mathfrak{M}_m(\theta)}{\chi_W(\theta)}\sin(\theta)\,d\theta + \bar{b}_T^3\sum_{\text{odd}}^{N} A_{T_n}\int_0^{\pi/2}\frac{\mathfrak{M}_n(\theta)}{\chi_T(\theta)}\sin(\theta)\,d\theta\right]$$

Our reference wing provides convenient standards for nondimensionalizing this expression. For this purpose, both its lift distribution and its planform are defined to be elliptical. The weight of the system relative to the reference wing may then be written as

$$W = f_S S + f_b\frac{b_W^3}{S}\left[\sum_{\text{odd}}^{M} A_{W_m}B_{W_m} + \bar{b}_T^3\sum_{\text{odd}}^{N} A_{T_n}B_{T_n}\right]$$

S, b_W, and W are now *relative* quantities. W_b and W_S have been replaced by f_b and f_S, which are the "spar" and "skin" weight fractions of the reference wing (note that $f_S = 1 - f_b$). The B coefficients are the same integrals that appeared earlier, except that they have been scaled so that $B_1 = 1$ for an elliptical surface.

Minimum Induced Drag with Fixed Weight and Area

Obviously, this approach is not the ultimate in structural analysis, but it does satisfy our requirement for an index that realistically accounts for the most powerful factors involved. We will now apply it to finding the minimum induced drag of a lifting system having fixed weight and area, rather than fixed span. Should the same lift distributions be used in the weight and drag calculations (apart from a load factor, which can be absorbed into f_b)? Not necessarily, but we shall see that minimizing drag at the maximum $-g$ C_L is a near-optimal strategy. If the same lift distributions determine both weight and drag, are those for optimum span efficiency, which were calculated in the preceeding section, still the best choice? Actually not, for carrying more lift inboard than is best for span efficiency reduces the integrated bending moments and thus allows a larger span for a fixed weight. Although the span efficiency u decreases, $(b_W^2 u)$—the quantity ultimately determining the drag—increases overall. Thus we must solve for minimum system drag with a weight constraint as a distinct problem. Actually this problem is very much in the spirit of those treated by Prandtl[7] and R. T. Jones[8,9] on minimum drag of a wing with fixed bending moment. Here we will present a solution extending these analyses in two respects: 1) it involves a weight model that is sensitive to variations in section thickness (through variations in chord) as well as to the moment distribution; and 2) it applies to a system of two interfering surfaces rather than an isolated monoplane. Appendix B gives the details of the analysis. One of its key features is that if the total area is fixed, then the "skin" term is no longer a variable and the solution becomes independent of the constants f_b and f_S. Hence, it depends only upon $\bar{S}_T$, $\bar{L}_T$, $\bar{b}_T$, $\bar{h}$, and, through the B coefficients, upon the planforms of the two surfaces.

The first four of these parameters entered into the trimmed drag calculations of the preceeding section, but the planforms are new elements. Naturally, we want nothing but the best, i.e., the planforms that offer the maximum span for a fixed weight or, equivalently, *minimum weight* for a fixed span. It turns out, upon differentiation of our formula for weight per unti span, that making the chord at each point proportional to the square root of the bending moment satisfies this condition. (This is true whether or not the total area is fixed; an area constraint simply scales the planforms.) Unfortunately, since the section lift does not *decrease* from root to tip as rapidly as does the bending moment, the corresponding section C_l is always very large over the outboard part of the surface—a situation that is obviously impractical. Aside from the limitations imposed by spanwise pressure gradients and parasite drag, one is generally forced to make the C_l over the outboard part of a wing *lower* than the average to avoid tip stall. The natural way to accommodate this constraint is to place an upper bound on C_l that varies across the span. Not surprisingly, the optimum chord then turns out to be

$$c(y) = \max\left(\frac{l(y)}{qC_{l_{\text{bound}}}},\ k\sqrt{M(y)}\right)$$

with k scaled to give the correct surface area.

Now the question becomes, what are reasonable bounds to place on C_l? Fortunately, the minimum drag solution is fairly insensitive to variations over the range of practical possiblities. Here we have used a constraint that varies linearly across the span, from 0.9 of the surface C_L at the tip to 1.2 at the root. Figure 6 shows the resulting minimum drag values. By comparison, systems with constant C_l across each surface have slightly higher drag than Fig. 6 indicates. At the

other extreme, if unbounded C_l really could be achieved, then the drag could be reduced by about 7% in aft-tailed systems and by 7-11% in canards. In any case, the relative positions of competing systems remain much the same as shown in Fig. 6. For the same weight, systems with large tail spans are, as anticipated, inferior to those with moderate tail spans. Also, systems with large tail areas are generally inferior to those with small tails.

Optimum Lift and Chord Distributions

While these results are not sensitive to the choice of C_l bounds, the effect of varying the lift distributions is marked. If for example the "maximum u" lift distributions are used rather than those for maximum $(b_W^2 u)$, then for the same weight the drag would be significantly higher across the board. The increment is particularly large for canard systems, as the following example will illustrate. Take a system having $\bar{S}_T = 0.4$ and $\bar{b}_T = 0.65$. (This is one of the systems whose "maximum u" lift distributions are plotted in Fig. 3. We will justify the choice of parameters later.) With $\Delta = 0.1$, its tail lift fraction is 0.53 and a span efficiency as high as 0.84 can be achieved, but only by making the wing's lift distribution very tip heavy. To satisfy the weight constraint with that high tip loading, the span would have to be relatively small—in fact, as indicated in Fig. 3, $b_W = 0.83$. Combining the number with the span efficiency gives a drag over 70% higher than that of the reference wing. Figure 7 illustrates a better strategy. Sloshing the wing's lift inboard reduces u to 0.73, but the span can be made *greater* than the reference wing's—1.03 to be precise. The corresponding drag is 28% higher than the reference value—hardly an impressive figure in itself, but quite an improvement over the alternative. If the gap were smaller, a higher u could be achieved, but only by increasing the tip loading. With the same lift distributions, the drag would actually be worse. For this reason, in this system and in fact all others with heavily loaded tails, the gap should be made as large as possible. $\bar{h} = 0.1$ is a rough upper limit for most canard arrangements.

However, whatever the gap, systems with lightly loaded tails have a substantial advantage over systems with heavy tail loading. These also benefit from the "maximum $(b_W^2 u)$" strategy. Consider, for example, an aft-tailed system with $\bar{S}_T = 0.2$ and $\bar{b}_T = 0.45$; $\bar{L}_T$ in this case is only 0.04. The drag with the "maximum u" lift distributions is 1.14, and with "maximum $(b_W^2 u)$" is 1.02. This is obviously a significant difference, and is about the same as Jones and Prandtl projected through the use of similar strategies.

The last number is particularly noteworthy since it compares favorably with the drag of our elliptical (and therefore nonoptimal) reference wing. Of course, the credit goes not only to the lift distributions but also to the surface planforms plotted in Fig. 8. These surfaces, as well as those in the canard system, have a characteristic shape: over the outboard section, the chord is set by the C_l bound and the contour follows the lift distribution. The area left over after the C_l constraint has been satisfied is concentrated inboard in a flared root similar to those of most transport wings. While the inboard sections should therefore have some familiar appeal, the practically minded will doubtless be skeptical of the curvaceous outboard contours and small tip chords. But these should not be taken as blueprints, any more than should Prandtl's elliptical wing. Rather, the real value of such an ideal solution is to define that which should be approximated in practice. Such approximations can give very nearly ideal performance.

Twist

Although the lift distributions and planforms plotted here are complementary elements of the "maximum $(b_W^2 u)$" solution, they are not matched in the purely aerodynamic sense. To prevent the lift distributions from becoming more tip heavy than the solution prescribes, each surface must be washed-out. At a C_L of 1, the aft-tailed system would need

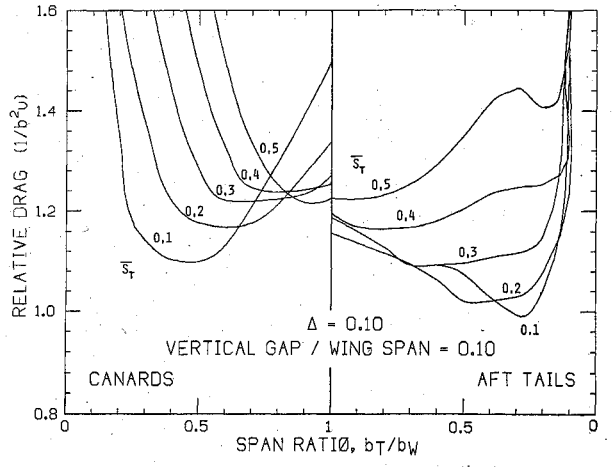

Fig. 6 Relative induced drag with fixed weight and surface area.

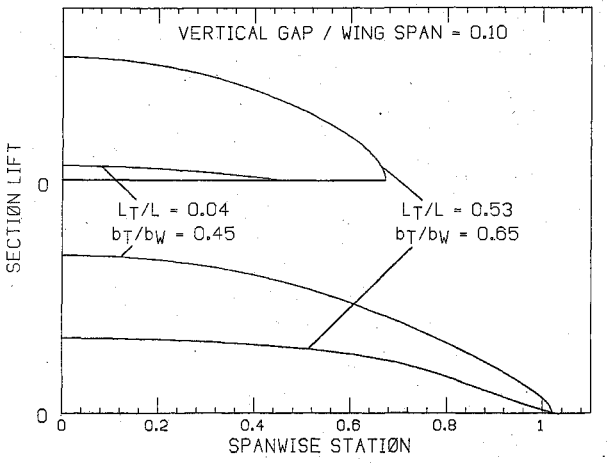

Fig. 7 Lift distributions for minimum drag with fixed weight.

about 5 deg in the wing and 2 deg in the tail, and the canard about 11 and 3 deg, respectively. The twist required scales with the design C_L. Unfortunately, variable twist wings are hard to build, so variations in their lift distributions with C_L must be accepted. Of course, whenever these change—not only with C_L, but also with $\bar{L}_T$—so does the span efficiency. It turns out that the span efficiency of a sytem with fixed twist is given by the quadratic,

$$\frac{1}{u} = \frac{1}{u_d} + k_1 \frac{\Delta C_L}{C_L} + k_2 \left(\frac{\Delta C_L}{C_L}\right)^2 + k_3 \Delta \bar{L}_T + k_4 \Delta \bar{L}_T^2 + k_5 \frac{\Delta C_L}{C_L} \Delta \bar{L}_T$$

where ΔC_L and $\Delta \bar{L}_T$ are deviations from the design values. Figure 9 shows this function for our two example systems in the form of contours of (u_d/u), which is just the ratio of the actual drag to that which the nominal lift distributions would give at the *same* C_L. Note that the C_L in the denominator is a variable, and *not* the design C_L. Thus, $+1$ on the $(\Delta C_L/C_L)$ scale corresponds to a C_L of ∞ and $-\infty$ to a C_L of 0.

Once the design lift distribution is specified, nothing can be done about the form of this function; thus, only the amount of twist to build in remains to be chosen. Actually, one would want to build in just enough twist to make the design C_L equal to that at which maximum g is encountered. The justification is as follows: if the surfaces had less twist, then in the critical condition their lift distributions would be more tip heavy than those for maximum $(b_W^2 u)$. (That is why the span efficiency improves at C_L above C_{L_d}.) Therefore, one would have to make the span less than optimal to satisfy the weight constraint and the result would be higher drag throughout the C_L range. On the other hand, suppose that the surfaces had more twist than was needed at the critical C_L. Since this C_L is normally near the "clean" $C_{L_{max}}$ of the system, it would make

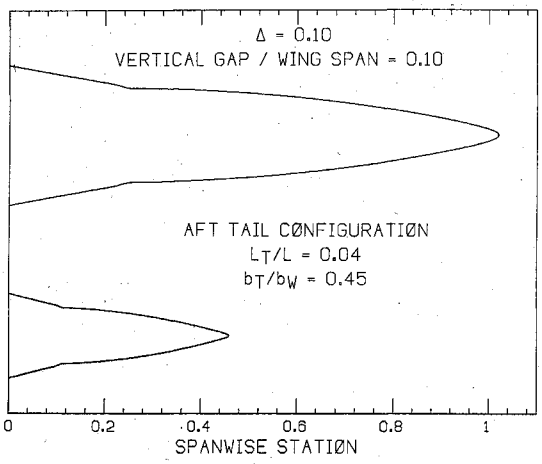

Fig. 8 Planforms for minimum drag with fixed weight.

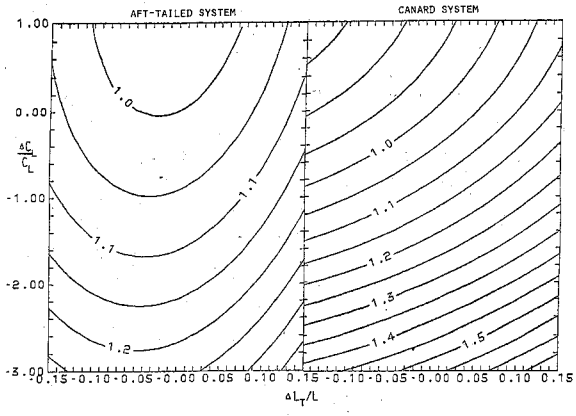

Fig. 9 Induced drag increment with deviations from design C_L and tail lift fraction.

the tip loading, and therefore the span efficiency, lower than optimal throughout the normal flight regime. Building in just enough for the critical condition minimizes the efficiency penalty.

Still, the penalty remains significant, which raises a question about our optimization scheme. What we have really found are the lift distributions that give minimum drag at the *design* C_L. Might it be better to adopt different design lift distributions, giving up some drag at this C_L in return for less sensitivity to C_L variations? Such distributions exist; in fact, systems designed for maximum u maintain essentially constant efficiency over the entire flight evelope. But it turns out that, in both of our example configurations, the "maximum $(b_W^2 u)$" design would retain its advantage down to low C_L. This strategy would therefore be superior overall and, in fact, so close to optimal that the difference is insignificant. However, systems with sweep or a lower aspect ratio are in general more sensitive to C_L variations, so they would warrant more detailed analysis.

Having established, then, that Fig. 9 is representative of the best that our example systems have to offer, let us make some comparisons between them. The most obvious difference is that the canard is more sensitive to C_L than is the aft-tailed system. This sensitivity is characteristic of canards (and so an exception to our remark that if the tail load is fixed, performance is mostly independent of its streamwise position). It is due to the induced velocity field behind the canard, which amplifies the variation of the wing's lift distribution with C_L. Since these induced velocities strengthen as the gap decreases, canards with small gaps are still more sensitive—50% more if the gap of our example system were halved. That same velocity field has a beneficial effect when the canard's lift fraction changes, since it shifts the wing's lift distribution toward that for maximum u. However, that is not very encouraging for stable canard systems, which, as we've seen, are quite sensitive to changing $\bar{L}_T$ even with the *best* lift distributions. In fact, this comparison bears much the same message as the rest of our results on induced drag—even at their best, other configurations have higher drag than the conventional arrangement. Furthermore, they are generally more sensitive to tail geometry, gap, C_L, C_{M_O}, c.g. position, etc. But of course one has to consider total drag, not just the induced component, before drawing firm conclusions about the relative efficiency of competing systems. Therefore, another major component, parasite drag, must be added to the analysis.

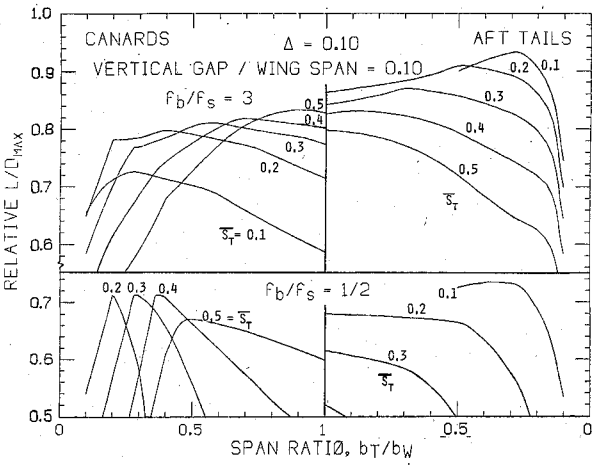

Fig. 10 Relative maximum L/D of trimmed systems with fixed weight and stall speed.

Parasite Drag and Total System Drag

Again, only the most important effects upon parasite drag should be included in the analysis. For this purpose, a simple parabolic expression for section C_d,

$$C_d = C_{d_0} + kC_l^2$$

suffices. Integrating this expression over the two surfaces gives the parasite drag of the system. Actually, of the two terms, the second is less important: it is small compared with the first at low C_L and with induced drag at high C_L. So for the moment we'll concentrate upon the effect of C_{d_0} exclusively. Of course, this term encourages one to make the surface area as small as possible. Most often, this is limited by a stall speed requirement—that is, for a given system weight, a lower bound on the product $(S \cdot C_{L_{\max}})$. It is through this product that differences in trimmed $C_{L_{\max}}$ are really manifested. With this idea in mind, we can now construct a basic measure of the relative efficiency of lifting systems, namely, total drag with a fixed weight and stall speed. With that measure, the question of which systems have the best combination of induced drag and $C_{L_{\max}}$ can be addressed. Since the ratio of induced to parasite drag increases with C_L, so will the performance of systems with high $(b_W^2 u)$ improve relative to those with high $C_{L_{\max}}$. However, comparing all systems at their *minimum* drag points (that is, at their maximum L/D) distinguishes the near-optimal from those that are inferior overall.

Relative L/D

Applying the usual procedure gives the maximum L/D of a system, relative to that of the reference wing, as

$$(L/D)_{\max} = \sqrt{b_W^2 u / S}$$

if u independent of C_L. The variation is ignored in this analysis, since it is of the same order as the C_L^2 term in the parasite drag. Now with fixed weight, b_W is a function of S. As Appendix B relates,

$$b_W^3 \sim \left[1 + \frac{f_S}{f_b}(1 - S)\right] S$$

This function has a maximum when $S=(1/2f_S)$; making the area smaller than that actually increases the induced drag at a given speed. Nevertheless, the smaller the area, the higher the L/D, according to

$$\left(\frac{L}{D}\right)_{\max}=\sqrt{(b_W^2u)_{S=1}}\left(1+\frac{f_S}{f_b}(1-S)\right)^{1/3}\frac{1}{S^{1/6}}$$

In order to evaluate this expression, a couple of parameters must be specified: 1) the ratio of the potential $C_{L_{\max}}$'s of the wing and tail, since it has some effect upon relative system $C_{L_{\max}}$ (the figure of 0.9 which was used earlier, is represen-tative); and 2) (f_b/f_S) for the *reference wing* (it will be lower for a system needing more area). L/D is fairly sensitive to this parameter, which ranges from less than ½ for some light aircraft to about 3 for a large transport. Plots of the L/D for both of these extreme cases are shown in Fig. 10.

First consider the case of $(f_b/f_S)=½$. The maximum wing span then corresponds to $S=¾$; since all systems need $S>1$ to satisfy the stall speed requirement, both parasite and induced drag suffer as $C_{L_{\max}}$ decreases. L/D is therefore quite sensitive to $C_{L_{\max}}$ variations and shows a similar variation with system geometry. In this case, the $C_{L_{\max}}$ advantage of the best canards roughly balances the higher (b_W^2u) of systems with small aft tails, so they have comparable L/D. As (f_b/f_S) increases, inferior $C_{L_{\max}}$ becomes less of a handicap and high (b_W^2u) more of an asset. Relative L/D therefore improvesuniversally, with high (b_W^2u) systems gaining on the rest. The optima among canards become broader and move toward higher span ratios. Among aft-tailed sytems the shift is toward lower span ratios, but less pronounced since $C_{L_{\max}}$ and induced drag do not conflict as strongly as in canards. The tail sizes for our example sytems were chosen because they are at least near optimal, as measured by the $(L/D)_{\max}$ index, over the range $1<(f_b/f_S)<3$. (We have, however, limited ourselves to an aft tail area of 0.2, since controllability would preclude making the tail much smaller.) Over this range the L/D of the aft-tailed system remains about 10% better than the canard's.

Complete Drag Polars

To illustrate the differences between these systems in more detail, their drag over the entire flight envelope must be compared. The variations in both u and parasite drag with C_L will be included in this comparison. First however, the latter particularly needs elaboration. Since parasite drag is a nonlinear function of C_l, variations in C_l across the spans and differences between the surface C_L's increase the drag. The penalty due to spanwise variations is negligible with the C_l constraint imposed here; it adds only about 1% to the kC_L^2 term. On the other hand, the penalty due to differences in the surface C_L's can be substantial. As far as this drag component is concerned, low tail loads (and correspondingly high wing C_l) are undesirable. The penalty is therefore normally larger in stable aft-tailed systems than in canards; in our examples, surface C_L discrepancies add 15 and 7%, respectively, to the kC_L^2 term.

Adding the components gives the total drag, in dimensional form, as

$$D=qSC_{d_0}+\frac{L^2}{\pi qb_W^2}\left[\frac{1}{u}+k\pi\mathcal{R}\left(\frac{\bar{L}_W^2}{\bar{S}_W}+\frac{\bar{L}_T^2}{\bar{S}_T}\right)\right]$$

where $\mathcal{R}$ is the overall aspect ratio. The term in parentheses accounts for differences between the surface C_L's; it is unity if they are equal. Now, it is convenient to nondimensionalize using the (qSC_{d_0}) term for the reference wing at some nominal dynamic pressure, say q_d. The result is that

$$\frac{D}{D_{\text{REF}}}=\frac{q}{q_d}S+\frac{\beta}{(q/q_d)b_W^2}\times\frac{\left[\frac{1}{u}+k\pi\mathcal{R}_{\text{REF}}\frac{b_W^2}{S}\left(\frac{\bar{L}_W^2}{\bar{S}_W}+\frac{\bar{L}_T^2}{\bar{S}_T}\right)\right]}{1+k\pi\mathcal{R}_{\text{REF}}}$$

These terms need some explanation. $(k\pi\mathcal{R}_{\text{REF}})$ is the ratio of the parasite and induced components of the "lift dependent" term in the drag polar of the reference wing. A typical value, which we will use here, is 0.2. β is the ratio of the reference wing's "lift-dependent" and "zero lift" terms at the nominal dynamic pressure. We take q_d to correspond with the design C_L; since this is fairly high, β will be large. For example, a wing having $\mathcal{R}_{\text{REF}}=8$ and $C_{d_0}=0.007$ will have $\beta=7$ at $C_L=1$ and $\beta=15$ at $C_L=1.5$. We'll use a representative value of 12. (The figure would be less for a complete airframe, of course.)

Figure 11 shows the resulting drag polars. With these parameters, the drag of the aft-tailed system remains about 5/6th of the canard's over a wide speed range. As it happens, these systems have the same trimmed $C_{L_{\max}}$ (if $C_{L_{\max W}}/C_{L_{\max T}}=0.9$), so this margin is independent of (f_b/f_S). However, (f_b/f_S) does have to be specified to scale the drag relative to that of the reference wing; the scaling here is for $(f_b/f_S)=1$.

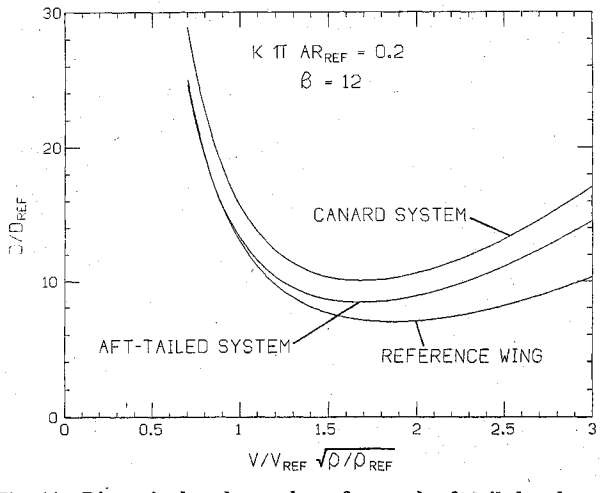

Fig. 11 Dimensionless drag polars of example aft-tailed and canard systems.

Conclusion

Given the drag polars plotted in Fig. 11, which system would you choose? There is nothing to debate—anyone would, without hesitation, dimiss *both* the canard and the aft-tailed system and embrace the reference wing! The clear inferiority of the two-surface systems is just the price that one pays for a moderate amount of stability and control. Simply stated, the stability requirement forces the center of gravity to be further forward and, this, in turn, causes the load on the forward surface to be larger than is optimal for either $C_{L_{\max}}$ or induced drag or, most often, both. Our analysis really amounts to a search for the geometry that makes the performance penalty as small as possible. We have found that to minimize the induced drag penalty, one is driven toward larger forward surface span and, to minimize the $C_{L_{\max}}$ penalty, one is driven toward larger forward surface area. (Since systems with very small aft tails have poor performance, this is true only to a point, but controllability limits the tail size before efficiency begins to suffer. Also those canard systems with equal C_L on both surfaces are exceptions, but their sensitivity and high induced drag are intimidating.) Thus, the conventional arrangement has a fundamental advantage among naturally stable lifting systems; an alternative arrangement could only be competitive in an application that permitted some offsetting economy in the overall layout of the airframe.

Recall that there is symmetry between stable canard systems and unstable aft-tailed systems. This implies that if Δ were

sufficiently negative, then the aft-tailed configuration would suffer the same penalties beseting stable canards. Hence, *both* negative and positive stability can be bad for efficiency; optimum efficiency must be achieved with some intermediate stability level. With relaxed static stability now in prospect, indentifying that level has become a hot issue. We can find it easily by reversing our analytical procedure. The idea is to treat the tail size and lift fraction as the independent variables and Δ as the dependent variable. The lift fraction fixes the c.g. postion and the size fixes the neutral point; Δ is just the distance between these points. Now, what are optimum values for the tail lift and tail size? One would want the tail to be as small as possible; the limit imposed by the control requirement is probably about $\bar{S}_T = 0.15$, $\bar{b}_T = \frac{1}{3}$. A near-optimal lift fraction for such a tail is 0.05. The corresponding Δ turns out to be 0.03, Thus, the optimum system is stable, which may come as a surprise. But remember that with the usual negative C_{M_O}, one would have to reduce Δ to achieve the specified tail load, and that a destabilizing fuselage term would further decrease the stability. Hence, the practical optimum is presumably about neutral. By applying the same reasoning to a canard configuration, we can conclude that its efficiency would be best with $\Delta = -0.03$, excluding downwash effects and other contributions to the pitching moment, and perhaps -0.1 with these included. This is obviously not an attractive alternative, since it offers no better efficiency than a more stable aft-tailed system.

While most our analysis is thus a hearty endorsement of conventional design practice dating back to Cayley, it does indicate room for significant improvement in one area—wing lift distributions. The familiar elliptical loading certainly does *not* give minimum induced drag for a fixed structural weight; we have calculated that one can do better by more than 10% even with a realistic wing twist and planform. Of course, this calculation is based upon a weight formula that is at best only good to first order. Would a more complete analysis give a similarly promising result? That is a question very much worth pursuing.

$$T = \begin{bmatrix} 3 & 0 & \cdots & 0 & T_{WT_{33}}/\bar{b}_T & T_{WT_{35}}/\bar{b}_T & \cdots & T_{WT_{3N}}/\bar{b}_T \\ 0 & 5 & \cdots & 0 & T_{WT_{53}}/\bar{b}_T & T_{WT_{55}}/\bar{b}_T & \cdots & T_{WT_{5N}}/\bar{b}_T \\ \vdots & \vdots & & \vdots & \vdots & \vdots & & \vdots \\ 0 & 0 & \cdots & M & T_{WT_{M3}}/\bar{b}_T & T_{WT_{M5}}/\bar{b}_T & \cdots & T_{WT_{MN}}/\bar{b}_T \\ T_{WT_{33}}/\bar{b}_T & T_{WT_{53}}/\bar{b}_T & \cdots & T_{WT_{M3}}/\bar{b}_T & 3/\bar{b}_T^2 & 0 & \cdots & 0 \\ T_{WT_{35}}/\bar{b}_T & T_{WT_{55}}/\bar{b}_T & \cdots & T_{WT_{M5}}/\bar{b}_T & 0 & 5/\bar{b}_T^2 & \cdots & 0 \\ \vdots & \vdots & & \vdots & \vdots & \vdots & & \cdots \\ T_{WT_{3N}}/\bar{b}_T & T_{WT_{5N}}/\bar{b}_T & \cdots & T_{WT_{MN}}/\bar{b}_T & 0 & 0 & \cdots & N/\bar{b}_T^2 \end{bmatrix}$$

Appendix A: Minimum Induced Drag of Systems with Fixed Span

The induced drag of two interfering surfaces in incompressible flow may be written as

$$D_i = \int_{\text{wing}} \epsilon_W l_W(y)\,dy + \int_{\text{tail}} \epsilon_T l_T(y)\,dy + \int_{\text{tail}} \epsilon_{WT} l_T(y)\,dy$$

where l represents the local lifts and ϵ the downwash angles. The terms are, respectively, the wing and tail "self-induced" drag and the interference drag. We have invoked Munk's stagger theorem to condense this term into a single integration over the tail; ϵ_{WT} is the downwash induced by wing's trailing vorticity at the tail's projection in the Trefftz plane. If the lift distributions are expressed as Fourier series, as in our derivation of the structural weight formula, then this expression becomes a summation,

$$D_i = \frac{L^2}{qb_W^2}\frac{\pi}{4}\left[\sum_{\text{odd}}^{M} mA_{W_m}^2 + \frac{1}{\bar{b}_T^2}\sum_{\text{odd}}^{N} nA_{T_n}^2 + \frac{2}{\bar{b}_T}\sum_{\text{odd}}^{M}\sum_{\text{odd}}^{N} A_{W_m}A_{T_n}T_{WT_{mn}}(\bar{b}_T,\bar{h})\right]$$

where $T_{WT_{mn}}$ accounts for the interference between the mth harmonic of the wing's lift distribution and the nth harmonic of the tail's. (Evaluation of the T_{WT} is somewhat involved; it requires a double integration.)

Our objective is to find the lift distributions, and therefore the circulation coefficients, which minimize the drag. However, A_{W_1} and A_{T_1} must be specified, since these are directly related to the surface lift fractions,

$$\bar{L}_W = \frac{\pi}{2}A_{W_1} \qquad \bar{L}_T = 1 - \bar{L}_W = \frac{\pi}{2}A_{T_1}$$

It is convenient to group the remaining free coefficients into a vector and then express the induced drag in matrix form. Thus, we define

$$\bar{A} = [A_{W_3}A_{W_5}\ldots A_{W_M}A_{T_3}A_{T_5}\ldots A_{T_N}]^T$$

and group the T_{WT} as

$$\bar{T}_{W_1} = [0\ 0\ldots 0\ T_{WT_{13}}T_{WT_{15}}\ldots T_{WT_{1N}}]^T/\bar{b}_T$$

$$\bar{T}_{T_1} = [T_{WT_{31}}T_{WT_{51}}\ldots T_{WT_{M1}}\ 0\ 0\ldots 0]^T/\bar{b}_T$$

Then the drag summation may be written as

$$D_i = \frac{L^2}{\pi q b_W^2}\left[\bar{L}_W^2 + \frac{\bar{L}_T^2}{\bar{b}_T^2} + \frac{2}{\bar{b}_T}\bar{L}_W\bar{L}_T T'_{WT_{11}} + \frac{\pi^2}{4}\bar{A}^T\left(T\bar{A} + \frac{4}{\pi}(\bar{L}_W\bar{T}_{W_1} + \bar{L}_T\bar{T}_{T_1})\right)\right]$$

The drag is least when the gradient of this expression, with respect to $\bar{A}$, is 0. After a bit of algebra, it emerges that $\bar{A}$ is then

$$\bar{A} = -1\frac{2}{\pi}T^{-1}(\bar{L}_W\bar{T}_{W_1} + \bar{L}_T\bar{T}_{T_1})$$

The indicated matrix multiplication produces two more vectors, which we'll denote by

$$\bar{\alpha}_W = -T^{-1}\bar{T}_{W_1} \qquad \bar{\alpha}_T = -T^{-1}\bar{T}_{T_1}$$

To find the induced drag generated by the corresponding lift distributions, this solution for $\bar{A}$ must be substituted back into the drag formula. The process is not detailed here because it is more tedious than tricky; however, it can be seen without any analysis that three terms will result: one proportional to $\bar{L}_W^2$, one to $\bar{L}_T^2$, and one to $\bar{L}_W\bar{L}_T$. Since $\bar{L}_W = (1 - \bar{L}_T)$, the result can also be written as a quadratic in $\bar{L}_T$ explicitly,

$$D_i = \frac{L^2}{\pi q b_W^2}\left[\sigma_0 + \frac{\sigma_{0T}}{\bar{b}_T}\bar{L}_T + \frac{\sigma_{TT}}{\bar{b}_T^2}\bar{L}_T^2\right]$$

The interference factors can be expressed in any of several ways (cf. Ref. 10); convenient forms are

$$\sigma_0 = 1 + \bar{\alpha}_W^T \cdot \bar{T}_{W_1}$$

$$\frac{\sigma_{0T}}{\bar{b}_T} = -2 + \frac{2T_{WT_{11}}}{\bar{b}_T} + (\bar{\alpha}_T - \bar{\alpha}_W)^T \cdot \bar{T}_{W_1} + \bar{\alpha}_W^T \cdot (\bar{T}_{T_1} - \bar{T}_{W_1})$$

$$\frac{\sigma_{TT}}{\bar{b}_T^2} = 1 + \frac{1}{\bar{b}_T^2} - \frac{2T_{WT_{11}}}{\bar{b}_T} + (\bar{\alpha}_T - \bar{\alpha}_W)^T \cdot (\bar{T}_{T_1} - \bar{T}_{W_1})$$

This solution using Fourier decomposition is exact if an infinite number of harmonics is included. But, practically, 1% accuracy can be obtained with only 5 harmonics in most cases, and even in the relatively extreme case of $\bar{h} = 0.05$, $\bar{b}_T = 0.1$, the solution is accurate to about 0.1% with 21 harmonics on the wing, and 5 on the tail.

Appendix B: Minimum Induced Drag with Fixed Weight

Here we will find the minimum drag that can be achieved with a given system weight. The analysis combines the procedure used in Appendix A with the weight formula derived in the text. The span ratio is a fixed parameter, as are the areas, lift fractions, and planforms of the two surfaces; the free variables are the wing span b_W and the higher harmonics of the lift distributions. The solution is obtained in two steps: 1) the optimum lift distributions, with the span as a parameter, and 2) the optimum span.

Again it is convenient to use matrix notation. If the B coefficients from the weight formula are grouped into a vector

$$\bar{B} = [B_{W_3} B_{W_5} \ldots B_{W_M}\ \bar{b}_T^3 B_{T_3} \bar{b}_T^3 B_{T_5} \ldots \bar{b}_T^3 B_{T_N}]^T$$

then the weight constraint can be expressed as

$$\frac{W - f_S S}{f_b} \frac{S}{b_W^3} \equiv \frac{\mu}{b_W^3} = \frac{2}{\pi} (\bar{L}_W B_{W_1} + \bar{b}_T^3 \bar{L}_T B_{T_1}) + \bar{A}^T \cdot \bar{B}$$

This constraint can be appended to the induced drag formula with a Lagrange multiplier ν. There is no need to include terms without $\bar{A}$ in the resulting expression, since they remain fixed; the variable part is

$$D' = \frac{1}{b_W^2} \bar{A}^T \left[T\bar{A} + \frac{4}{\pi} (\bar{L}_W \bar{T}_{W_1} + \bar{L}_T \bar{T}_{T_1}) \right] + \nu \left(\frac{2}{\pi} (\bar{L}_W B_{W_1} + \bar{b}_T^3 \bar{L}_T B_{T_1}) + \bar{A}^T \cdot \bar{B} - \frac{\mu}{b_W^3} \right]$$

As before, the optimum $\bar{A}$ vector is found by setting the gradient of D' to 0. The solution is that

$$\bar{A} = -\frac{2}{\pi} T^{-1} (\bar{L}_W \bar{T}_{W_1} + \bar{L}_T \bar{T}_{T_1}) - \frac{b_W^2 \nu}{2} T^{-1} \bar{B}$$

which includes the $\bar{\alpha}$ vectors that arose earlier and a third denoted by

$$\overline{\Delta\alpha} = -T^{-1} \bar{B}$$

The Lagrange multiplier [or, more conveniently, $(b_W^2 \nu/2)$,] is determined by substituting $\bar{A}$ back into the weight constraint. Some algebra yields

$$\frac{b_W^2 \nu}{2} = \frac{\frac{\mu}{b_W^3} - \frac{2}{\pi} \bar{L}_W (B_{W_1} + \bar{\alpha}_W^T \cdot \bar{B}) - \frac{2}{\pi} \bar{L}_T (\bar{b}_T^3 B_{T_1} + \bar{\alpha}_T^T \cdot \bar{B})}{\overline{\Delta\alpha}^T \cdot \bar{B}}$$

Notice that when (μ/b_W^3) has the same value as the vector term in the numerator—let us call that value (μ/b_W^{*3})—the Lagrange multiplier vanishes. In that case the wight constraint is satisfied by the maximum u lift distributions. As (μ/b_W^3) varies, the lift distributions change according to

$$\bar{A} = \frac{2}{\pi} (\bar{L}_W \bar{\alpha}_W + \bar{L}_T \bar{\alpha}_T) + \frac{1}{\overline{\Delta\alpha}^T \cdot \bar{B}} \left(\frac{\mu}{b_W^3} - \frac{\mu}{b_W^{*3}} \right) \overline{\Delta\alpha}$$

The corresponding variation in drag can be found by substituting this result into the drag formula. After some manipulation, one obtains the following explicit relationship between induced drag and span:

$$D_i = \frac{L^2}{\pi q b_W^2} \left[\sigma_0 + \frac{\sigma_{0T}}{\bar{b}_T} \bar{L}_T + \frac{\sigma_{TT}}{\bar{b}_T^2} \bar{L}_T^2 - \frac{\pi^2}{4} \frac{1}{\overline{\Delta\alpha}^T \cdot \bar{B}} \left(\frac{\mu}{b_W^3} - \frac{\mu}{b_W^{*3}} \right)^2 \right]$$

At this point the second step of the solution procedure (finding the optimum span) would appear to involve no more than differentiating this expression with respect to b_W. But that approach holds some surprises. More often than not, this function does *not* have a minimum. And, even when it does, the minimum is only local; the drag becomes arbitrarily small by $b_W \to \infty$. This peculiar behavior is due to a limitation in our weight formula. In calculating the B coefficients back in the section on weight, we tacitly assumed that the bending moment does not change sign over the span of either surface. If that assumption is violated—as, for example, when the wing has negatively loaded tips—then the "spar" weight is counted as *negative* over some part of the span. As the span increases from b_W^*, a point is reached at which this transition occurs; beyond that point our analysis no longer applies. But the tantalizing observation is that the *derivative* is often negative at the transition point; hence, negative tip loading really would be optimal for many systems. However, the practicality of negative tip loading is obviously debatable; rather than join that debate here, we have simply compared systems using the minimum drag achievable with positive loading everywhere. Thus, we have taken the optimum span for any system to be that at the transition point, or, if it has one, that at the local minimum in the positive-loading range. Actually, both of these points correspond to characteristic values of μ/b_W^3, rather than b_W itself. Hence, the span scales with μ according to

$$b_W^3 = \frac{1}{(\mu/b_W^3)_{\text{opt}}} \frac{W - f_S S}{f_b} S$$

Note that, if $W = S = 1$, then the optimum span is independent of f_b and f_S.

References

[1] von Kármán, Th. and Burgers, J. M., "General Aerodynamic Theory—Perfect Fluids," *Aerodynamic Theory*, Vol. II, edited by W. F. Durand, Dover Publications, New York, 1963.

[2] Feistal, T., Corsiglia, V., and Levin, D., "Wind-Tunnel Measurements of Wing-Canard Interference and a Comparison with Various Theories," SAE Paper 810575, April 1981.

[3] Blackwell, J., "Numerical Method to Calculate the Induced Drag or Optimal Loading for Arbitrary Non-Planar Aircraft," NASA SP-405, May 1976.

[4] Lamar, J. E., "A Vortex Lattice Method for the Mean Camber Shapes of Trimmed Non-Coplanar Planforms with Minimum Vortex Drag," NASA TN-D 8090, 1976.

[5] Butler, G. F., "Effect of Downwash on the Induced Drag of Canard—Wing Combinations," *Journal of Aircraft*, Vol. 19, May 1982, pp. 410-411.

[6] Kroo, I. M., "Minimum Induced Drag of Canard Configurations," *Journal of Aircraft*, Vol. 19, Sept. 1982, pp. 792-794.

[7] Prandtl, L., "Über Tragflugel des Kleinsten Induzierten Widerstandes," *Zeitshrift für Flugtechnik und Motorluftschiffahrt*, 24 Jg. 1933 (reprinted in Tollmein, W., Schlichting, H., and Gortler, H., eds., *Gesammelte Abhandlungen*, Springer-Verlag, Berlin, 1961.)

[8] Jones, R. T., "The Spanwise Distribution of Lift for Minimum Induced Drag of Wings Having a Given Lift and Root Bending Moment," NACA TN-2249, 1950.

[9] Jones, R. T. and Lasinski, T. A., "Effect of Winglets on the Induced Drag of Ideal Wing Shapes," NASA TM 81230, 1980.

[10] Kroo, I. M. and McGeer, T., "Optimization of Canard Configurations—An Integrated Approach and Practical Drag Estimation Method," *Proceedings of the 13th Congress of the International Council of the Aeronautical Sciences, Aug. 1982, pp. 1459-1469.*